Characterizing the dynamics of quantum discord under phase damping with POVM measurements*

Jiang Feng-Jian(蒋峰建)†, Ye Jian-Feng(叶剑锋), Yan Xin-Hu(闫新虎), and Lü Hai-Jiang(吕海江)‡

School of Information Engineering, Huangshan University, Huangshan 245041, *China*

(Received 13 February 2015; revised manuscript received 25 May 2015; published online 20 August 2015)

In the analysis of quantum discord, the minimization of average entropy traditionally involved over orthogonal projective measurements may be attained at more optimal decompositions by using the positive-operator-valued measure (POVM) measurements. Taking advantage of the quantum steering ellipsoid in combination with three-element POVM optimization, we show that, for a family of two-qubit X states locally interacting with Markovian non-dissipative environments, the decay rates of quantum discord show smooth dynamical evolutions without any sudden change. This is in contrast to two-element orthogonal projective measurements, in which case the sudden change of the decay rates of quantum and classical decoherences may be a common phenomenon. Notwithstanding this, we find that a subset of X states (including the Bell diagonal states) involving POVM optimization can still preserve the sudden change character as usual.

Keywords: quantum steering ellipsoid, quantum discord, decoherence

PACS: 03.65.Yz, 03.65.Ta, 89.70.Cf **DOI:** 10.1088/1674-1056/24/10/100304

1. Introduction

Quantum correlation can exist even without entanglement.[1] This deducing was further presented independently by Henderson *et al.*[2] and Ollivier *et al.*,[3] who demonstrate that, the two equivalent definitions of classical mutual information entropy can be generalized to the quantum version.[4] In the quantum case of composite systems $\mathscr{A}$ and $\mathscr{B}$, the Shannon entropy was replaced by the von Neumann entropy, for which the corresponding probability distributions are obtained from the density matrices. The differences of total and classical correlations associate with the to-be-measured set[3] of one system ($\mathscr{A}$ or $\mathscr{B}$). They defined the minimal difference called quantum discord $\mathscr{Q}$ as a measure for the quantum correlation, which has always been nonnegative and is zero for states with only classical correlations. The idea of discord provides a clue for DQC1 algorithm,[5] in which the quantum correlation scales with quantum efficiency.[6] It is a starting point for applying discord to study many different protocols and problems[7–9] in quantum information processes. More significantly, what we want to know is to what extent the discord will be responsible for some quantum enhancements.[10,11] Following the definition of discord, various measures of quantum correlation in terms of optimal procedures are defined, such as quantum deficit,[12] geometric,[13–16] and relative entropy measures.[17]

The quantum discord, as a measure to quantify the quantum correlation, can capture much more non-classical correlation than that of the entanglement measure. Meanwhile, the dynamical evolutions of quantum discord under the Markovian and non-Markovian noises have also been investigated in Refs. [18]–[21]. It is shown that discord, contrary to entanglement, behaves much more robustly in resisting decoherence. In addition, the dynamics of discord conducted by non-dissipative Markovian environments result in a variety of interesting decoherence phenomena,[22–29] in which a freeze and sudden transition of classical and quantum correlation dynamics can emerge for the Bell diagonal states of two qubit states. The sudden transition behaviors show that the quantum and classical correlations remain constant and unaffected by decoherence before and after the transition point, respectively, while the sudden change behaviors just mean that the dynamics of quantum and classical correlations are non-smooth. Obviously, the behaviors of the sudden transition are included in the cases of the sudden change.

It has been known that the sudden change behaviors result from the minimization procedure over the complete set of orthogonal projective measurements. Furthermore, the sudden change point can be reflected in the detailed calculation, in which the minimization will give rise to a non-smooth decay rate of discord due to the different choices of optimal observables.[30] Nevertheless, the minimization procedures involved over all possible measurements bring some difficulties in the analysis of discord. For bipartite mixed states, the analytical solution for the three-parameter family of Bell diagonal states was first obtained in Ref. [31], and lately Ali *et al.*[32] attempted to generalize the analytic form to the X states, in which the optimal observable is limited to a set of Pauli operators. Recently, researchers[33–35] have made clear that the

*Project supported by the National Natural Science Foundation of China (Grant Nos. 11305074, 11135002, and 11275083).

†Corresponding author. E-mail: jfjiang@mail.ustc.edu.cn

‡Corresponding author. E-mail: luhj9404@mail.ustc.edu.cn

© 2015 Chinese Physical Society and IOP Publishing Ltd

optimization for some two-qubit X states is state-dependent and out of the finite set as mentioned above. Meanwhile, the authors[36–40] found that, in the cases of POVM measurements, the minimization procedures may lead to more optimal quantities of discord than that given by orthogonal measurements for a family of X states.

In this paper, by using the visualized tool of the quantum steering ellipsoid,[41] we show that choosing three-element POVM measurements rather than orthogonal ones to analyze discord and classical correlation may obtain more optimal quantities for a family of X states. Furthermore, we find that, for some initial X states undergoing two-sided phase damping (PD), the dynamics of discord and classical correlation in the optimization over three-element POVM measurements exhibit two smooth evolving curves without any sudden change point, in contrast to the cases of the two-element orthogonal measurements. However, for the Bell diagonal states it turns out that the two alternative optimal procedures would lead to the same dynamics of discord and classical correlation, and that the sudden change point still exists.

2. The relationship of quantum discord and steering ellipsoid

For a bipartite quantum system $\rho_{\mathscr{A}\mathscr{B}}$, the quantum discord $\mathscr{Q}^{\leftarrow}_{\mathscr{A}\mathscr{B}}$ defined by the difference of total correlation $\mathscr{I}(\rho_{\mathscr{A}\mathscr{B}}) = \mathscr{S}(\rho_{\mathscr{A}}) + \mathscr{S}(\rho_{\mathscr{B}}) - \mathscr{S}(\rho_{\mathscr{A}\mathscr{B}})$ and classical correlation $\mathscr{C}^{\leftarrow}(\rho_{\mathscr{A}\mathscr{B}}) = \mathscr{S}(\rho_{\mathscr{A}}) - \min\sum_i p_i \mathscr{S}(\rho_{\mathscr{A}|M_i^{\mathscr{B}}})$ can be written as

$$\begin{aligned}\mathscr{Q}^{\leftarrow}_{\mathscr{A}\mathscr{B}} &= \mathscr{I}(\rho_{\mathscr{A}\mathscr{B}}) - \mathscr{C}^{\leftarrow}(\rho_{\mathscr{A}\mathscr{B}}) \\ &= \mathscr{S}(\rho_{\mathscr{B}}) - \mathscr{S}(\rho_{\mathscr{A}\mathscr{B}}) + \min\sum_i p_i \mathscr{S}(\rho_{\mathscr{A}|M_i^{\mathscr{B}}}), \quad (1)\end{aligned}$$

where $S(\rho) = -\mathrm{Tr}\rho\log_2\rho$ is the von Neumann entropy and in the quantum case the minimum is taken over a complete set of POVMs $\{M_i^{\mathscr{B}}\}$ on $\mathscr{B}$ with $p_i = \mathrm{Tr}[M_i^{\mathscr{B}}\rho_{\mathscr{A}\mathscr{B}}]$ and $\rho_{\mathscr{A}|M_i^{\mathscr{B}}} = \mathrm{Tr}_{\mathscr{B}}[M_i^{\mathscr{B}}\rho_{\mathscr{A}\mathscr{B}}]/p_i$. In general, $\mathscr{Q}$ is asymmetric, i.e., $\mathscr{Q}^{\rightarrow} \neq \mathscr{Q}^{\leftarrow}$, with $\mathscr{Q}^{\rightarrow}$ given by swapping the roles of $\mathscr{A}$ and $\mathscr{B}$. Exhausting all possible measurements can achieve the minimal average entropy

$$\overline{\mathscr{S}}_{\min} = \min\sum p_i \mathscr{S}(\rho_{\mathscr{A}|M_i^{\mathscr{B}}}) \quad (2)$$

in Eq. (1). For convenience of analysis, we only consider a class of X states with positive real matrix elements

$$\rho_{\mathscr{A}\mathscr{B}} = \begin{pmatrix} \rho_{11} & 0 & 0 & \rho_{14} \\ 0 & \rho_{22} & \rho_{23} & 0 \\ 0 & \rho_{32} & \rho_{33} & 0 \\ \rho_{41} & 0 & 0 & \rho_{44} \end{pmatrix}, \quad (3)$$

for which the positivity requires $\rho_{14}^2 \leq \rho_{11}\rho_{44}$ and $\rho_{23}^2 \leq \rho_{22}\rho_{33}$ with $\rho_{14} = \rho_{41}$ and $\rho_{23} = \rho_{32}$.

With the aid of a geometric picture of the steering ellipsoid abbreviated as $\mathfrak{E}$, one can visualize the optimal measurement of interest through finding an optimal convex combination of post-measurement ensemble $\rho_{\mathscr{A}} = \sum_k p_k \rho_k^{\mathscr{A}}$ in the $\mathfrak{E}$ (including the surface). It has been pointed out in Ref. [30] that any one element $\rho_k^{\mathscr{A}}$ of the optimal ensemble can only be found on the surface of $\mathfrak{E}$. Now let us define a 4×4 real matrix R with elements $R_{\mu\nu}$ given by $R_{\mu\nu} = \mathrm{Tr}\left[\rho_{\mathscr{A}\mathscr{B}}(\sigma_\mu \otimes \sigma_\nu)\right]$ for $\mu,\nu = 0,1,2,3$, where σ_0 is the identity matrix and $\sigma_{\mu(\nu)}$ $(\mu,\nu = 1,2,3)$ denote the usual Pauli matrices $\sigma_{x,y,z}$. Let a single-qubit positive operator $E_k = \boldsymbol{n}_k\cdot\boldsymbol{\sigma} = n_{k_0}\mathbb{I} + n_{k_1}\sigma_1 + n_{k_2}\sigma_2 + n_{k_3}\sigma_3$ be an element of general POVM set $\{E_k\}$ such that $n_{k_0}^2 \geq n_{k_1}^2 + n_{k_2}^2 + n_{k_3}^2$ and $n_{k_0} \geq 0$. For any point on the surface of $\mathfrak{E}$, the vector $\boldsymbol{n}_k$ satisfying $n_{k_0}^2 = n_{k_1}^2 + n_{k_2}^2 + n_{k_3}^2$ leads to a rank-1 POVM on $\mathscr{B}$.[30] In the Bloch vector representation, the matrix R acted by the POVM measurement is represented by

$$p_k \boldsymbol{V}_k = R\boldsymbol{n}_k,$$

where $\boldsymbol{V}_k = (1, x_k, y_k, z_k)^{\mathrm{T}}$ is the four-component vector of normalized marginal state $\rho_{\mathscr{A}}^k = \mathrm{Tr}_{\mathscr{B}}(E_k\rho_{\mathscr{A}\mathscr{B}})/\mathrm{Tr}(E_k\rho_{\mathscr{A}\mathscr{B}}) = \boldsymbol{V}_k\cdot\boldsymbol{\sigma}/2$, and $p_k = \mathrm{Tr}(E_k\rho_{\mathscr{A}\mathscr{B}}) = \sum_{\alpha=0}^{3} R_{0\alpha}n_{k_\alpha}$. The created ensemble $\{p_k, \boldsymbol{V}_k\}$ by POVM measurements would be constrained by

$$\boldsymbol{V}_k^{\mathrm{T}}[R^{-\boldsymbol{T}}\eta R^{-1}]\boldsymbol{V}_k \geq 0, \quad (4)$$

where the Minkowski metric tensor $\eta = \mathrm{diag}[1,-1,-1,-1]$. One can write out its steering ellipsoid equation[30]

$$\frac{x^2}{\ell_1^2} + \frac{y^2}{\ell_2^2} + \frac{(z-z_0)^2}{\ell_3^2} = 1, \quad (5)$$

where the three semi-axis lengths along the x, y, z axes and the location of the center of the $\mathfrak{E}$ correspond to

$$\begin{aligned}\ell_1 &= \frac{\rho_{14}+\rho_{23}}{\sqrt{(\rho_{11}+\rho_{33})(\rho_{22}+\rho_{44})}}, \\ \ell_2 &= \frac{|\rho_{14}-\rho_{23}|}{\sqrt{(\rho_{11}+\rho_{33})(\rho_{22}+\rho_{44})}}, \\ \ell_3 &= \frac{|\rho_{11}\rho_{44}-\rho_{22}\rho_{33}|}{(\rho_{11}+\rho_{33})(\rho_{22}+\rho_{44})}, \\ z_0 &= \frac{\rho_{11}\rho_{22}-\rho_{33}\rho_{44}}{(\rho_{11}+\rho_{33})(\rho_{22}+\rho_{44})}, \end{aligned} \quad (6)$$

respectively. The reduced state ρ_A corresponds to point A as shown in Fig. 2(a), and its Bloch vector is $(0,0,R_z)$ with $R_z = \rho_{11}+\rho_{22}-\rho_{33}-\rho_{44}$. The decomposed ensemble $\{p_k, \rho_{\mathscr{A}}^k\}$ of $\rho_{\mathscr{A}}$ distributing on the surface of three-dimensional $\mathfrak{E}$ brings out some inconveniences for finding the optimal $\overline{\mathscr{S}}_{\min}$. Concerning this case, we find that the optimal measurements for the X states must lie in the x–z plane.[37] So the following discussion is restricted to the ellipse abbreviated as E within the x–z plane (See Fig. 1(a)).

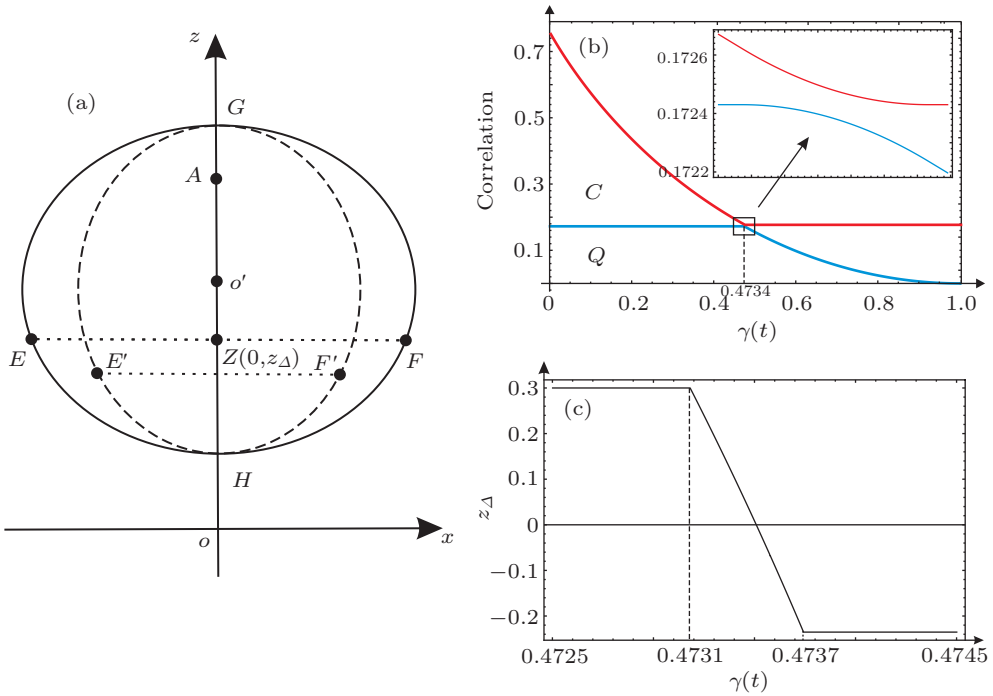


Fig. 1. (color online) (a) An E shrinks to z axis under the PD channels, and the E of the dashed line corresponds to the shrinking ellipse. Points G, E (E'), and F (F') represent the decomposed states respectively corresponding to a fixed point A under the POVM measurements. (b) Plot of the evolution of quantum and classical correlations of the X state with matrix elements $\rho_{11} = 0.4875$, $\rho_{22} = 0.1625$, $\rho_{33} = 0.0875$, $\rho_{44} = 1-\rho_{11}-\rho_{22}-\rho_{33}$, $\rho_{23} = 0.1118$, and $\rho_{14} = 0.3354$. The red and blue lines respectively correspond to classical and quantum decoherences. The time instant of $\gamma_C(t_0) \approx 0.4734$ corresponding to the sudden change point as the result of the two-element orthogonal measurements can make $\overline{\mathscr{S}}_{\leftrightarrow} = \overline{\mathscr{S}}_{\updownarrow}$. The embedded figure shows clearly that there is no sudden change point due to the optimization procedure of three-element POVM measurements. (c) Adopting the POVM optimization, the point $\mathscr{Z}$ can decrease continuously from point A to lower vertex H with the shrinking E.

A horizontal chord passing through the point A intersects with E, on which the two crossing points of E and F correspond to the decomposed two states induced by the two-element projective measurements $(I \pm \sigma_x)/2$ acting on partition $\mathscr{B}$ with probabilities $p_E = p_F = 1/2$. The coordinates of E and F are $\left(\pm \ell_1 \sqrt{\ell_3^2 - (R_z - z_0)^2}/\ell_3,\ R_z\right)$ in the x–z plane, respectively. The average entropy $\overline{\mathscr{S}}_{\leftrightarrow}$ given by a convex combination of $\mathscr{S}(\rho_E)$ and $\mathscr{S}(\rho_F)$ is

$$\begin{aligned} \overline{\mathscr{S}}_{\leftrightarrow} &= p_E\, \mathscr{S}(\rho_E) + p_F\, \mathscr{S}(\rho_F) \\ &= \mathscr{S}(\rho_E) = \mathscr{S}(\rho_F) = h(r), \end{aligned} \tag{7}$$

where

$$h(x) = -\frac{1-x}{2}\log_2\frac{1-x}{2} - \frac{1+x}{2}\log_2\frac{1+x}{2}$$

for $x \in [0,1]$ is a binary entropy function and

$$r = \overline{OE} = \overline{OF} = \sqrt{R_z^2 + \ell_1^2\,[\ell_3^2 - (R_z - z_0)^2]/\ell_3^2}.$$

Similarly, the average entropy $\overline{\mathscr{S}}_{\updownarrow}$ of vertical decomposition through the point A is

$$\begin{aligned} \overline{\mathscr{S}}_{\updownarrow} &= p_G\, \mathscr{S}(\rho_G) + p_H\, \mathscr{S}(\rho_H) \\ &= p_G\, h(\overline{OG}) + p_H\, h(\overline{OH}), \end{aligned} \tag{8}$$

where

$$p_G = \frac{\overline{AH}}{\overline{GH}}, \quad p_H = \frac{\overline{AG}}{\overline{GH}} = 1 - p_G.$$

The intersections of E and z axis correspond to the two vertices of G and H, whose coordinates are labeled as $(0, z_G)$ and $(0, z_H)$, respectively.

3. Local filtering operation

Specifically, introducing a local filtering operation (LFO)[39,40] of the form

$$F_{\mathscr{B}} = \begin{pmatrix} \sqrt{\alpha} & 0 \\ 0 & \sqrt{\beta} \end{pmatrix} \tag{9}$$

satisfies $F_{\mathscr{B}}^{\dagger} F_{\mathscr{B}} \leq \mathbb{I}$, where α and β are real positive values. Its action on the $\mathscr{B}$ of $\rho_{\mathscr{A}\mathscr{B}}$ can be represented by

$$\rho'_{\mathscr{A}\mathscr{B}} = \frac{(\mathbb{I}\otimes F_{\mathscr{B}})\rho_{\mathscr{A}\mathscr{B}}(\mathbb{I}\otimes F_{\mathscr{B}})^{\dagger}}{\mathrm{tr}[(\mathbb{I}\otimes F_{\mathscr{B}})\rho_{\mathscr{A}\mathscr{B}}(\mathbb{I}\otimes F_{\mathscr{B}})^{\dagger}]}. \tag{10}$$

In the Bloch vector representation, equation (10) can be transformed to

$$R' = \frac{1}{p} R \Lambda_{\mathscr{B}}^{\mathrm{T}}, \tag{11}$$

where $p = \mathrm{tr}[(\mathbb{I}\otimes F_{\mathscr{B}})\rho_{\mathscr{A}\mathscr{B}}(\mathbb{I}\otimes F_{\mathscr{B}})^{\dagger}]$, $\Lambda_{\mathscr{B}} = \Upsilon(F_{\mathscr{B}} \otimes F_{\mathscr{B}}^{*})\Upsilon^{\dagger}$ and

$$\Upsilon = \frac{1}{\sqrt{2}} \begin{pmatrix} 1 & 0 & 0 & 1 \\ 0 & 1 & 1 & 0 \\ 0 & \mathrm{i} & -\mathrm{i} & 0 \\ 1 & 0 & 0 & -1 \end{pmatrix}.$$

Under LFO, the $\mathfrak{E}$ remains invariant and the three semi-axis lengths and the location of center will be the same as Eq. (6),

whereas the Bloch vector of $\rho_{\mathscr{A}}$ steered by the LFO on $\mathscr{B}$ can be moved along the z axis. The Bloch vector of the steered reduced state $\rho_{\mathscr{A}}$ is then defined as $(0, r_z)$ in the x–z plane with the variable

$$r_z = \frac{(\rho_{11}-\rho_{33})+(\rho_{22}-\rho_{44})\beta/\alpha}{(\rho_{11}+\rho_{33})+(\rho_{22}+\rho_{44})\beta/\alpha}. \tag{12}$$

Consequently, we have

$$\begin{aligned} r_z &= \frac{\rho_{11}-\rho_{33}}{\rho_{11}+\rho_{33}}, \quad \text{for } \beta/\alpha \to 0, \\ r_z &= \frac{\rho_{22}-\rho_{44}}{\rho_{22}+\rho_{44}}, \quad \text{for } \beta/\alpha \to \infty \end{aligned} \tag{13}$$

corresponding to the σ_z component of G or H in the Bloch representation, respectively. Thus, the σ_z component of $\rho_{\mathscr{A}}$ can range along the entire line segment between the vertices of G and H.

4. The optimization of minimum average entropy using three-element POVM measurements

Remark 1 When the ellipse center is located at the origin, the function $\overline{\mathscr{S}}_{\leftrightarrow}(r_z)$ of horizontal decomposition defined by LFO is either concave or convex and has no inflexion point.

Immediately, one can reduce Eq. (8) to $\overline{\mathscr{S}}^{A}_{\updownarrow}(r_z) = \mathscr{S}(\rho_G) = \mathscr{S}(\rho_H) = h(\ell_3)$. For a fixed E with $z_0 = 0$, the z axis coordinate R_z of the local state ρ_A can be shifted along the z axis by LFO. Since the moved ρ_A is always on the z axis and $r_z \in (z_H, z_G)$, for $\ell_1 < \ell_3$ one can get $\overline{OE} < \ell_3$ resulting in $\overline{\mathscr{S}}_{\leftrightarrow}(r_z) > h(\ell_3)$, otherwise, for $\ell_1 > \ell_3$, $\overline{OE} > \ell_3$ resulting in $\overline{\mathscr{S}}_{\leftrightarrow}(r_z) < h(\ell_3)$.

The two functions of $\overline{\mathscr{S}}^{A}_{\leftrightarrow}(r_z)$ and $\overline{\mathscr{S}}^{A}_{\updownarrow}(r_z)$ never have any crossing point except for the two vertices G and H of E. We will demonstrate, in the following discussion, that there exists no inflection point for the function of $\overline{\mathscr{S}}_{\leftrightarrow}(r_z)$. Considering the second derivative of the entropy function $\overline{\mathscr{S}}_{\leftrightarrow}(r_z)$ with respect to r_z, one can get

$$\frac{\mathrm{d}^2\overline{\mathscr{S}}_{\leftrightarrow}(r_z)}{\mathrm{d}r_z^2} = -\frac{r''\operatorname{arctanh}(r)}{\ln 2} - \frac{r'^2}{\ln 2(1-r^2)}, \tag{14}$$

where $r' = \mathrm{d}r/\mathrm{d}r_z = (\ell_3^2-\ell_1^2)\, r_z/\ell_3^2\, r$ and

$$r'' = \frac{\mathrm{d}^2 r}{\mathrm{d}r_z^2} = \frac{(\ell_3^2-\ell_1^2)\left[\, \ell_3^2\,(r^2-r_z^2)+\ell_1^2\, r_z^2\,\right]}{\ell_3^4\, r^3}$$

with $r = \sqrt{r_z^2 + \dfrac{\ell_1^2(\ell_3^2-r_z^2)}{\ell_3^2}}$.

(i) For $\ell_1 > \ell_3$, one can obtain an inequality

$$\frac{\mathrm{d}^2\overline{\mathscr{S}}_{\leftrightarrow}(r_z)}{\mathrm{d}r_z^2} > -\frac{r r''}{\ln 2} - \frac{1}{\ln 2}\frac{r'^2}{1-r^2} > 0, \tag{15}$$

where the inequality (15) follows the Taylor expansion of $\operatorname{arctanh}(r) = \sum_{n=0}^{\infty} \frac{r^{2n+1}}{2n+1} > r$ for $r \in [0,1)$.

(ii) For $\ell_1 < \ell_3$, similarly one can get

$$\frac{\mathrm{d}^2\overline{\mathscr{S}}_{\leftrightarrow}(r_z)}{\mathrm{d}r_z^2} < 0. \tag{16}$$

Thus the function of $\overline{\mathscr{S}}_{\leftrightarrow}(r_z)$ is either concave or convex.

Having proved that, for the trivial case of $\ell_1 < \ell_3$ with $z_0 = 0$, the function of $\overline{\mathscr{S}}_{\leftrightarrow}(r_z)$ is concave, and the vertical decomposition can take the minimal value $\overline{\mathscr{S}}_{\min} = h(\ell_3)$. While $\ell_1 > \ell_3$, horizontal decomposition takes over and there exists no other optimal convex combination to achieve the minimum. For an extreme case of $\ell_1 = \ell_3$, any decomposition through the point A must be isotropic and give the same value of $\overline{\mathscr{S}}_{\min}$. Thus, the two functional curves of $\overline{\mathscr{S}}_{\updownarrow}(r_z)$ and $\overline{\mathscr{S}}_{\leftrightarrow}(r_z)$ of interest coincide with each other. So far, it can be safely said that, for the X states with $\rho_{11}\rho_{22} = \rho_{33}\rho_{44}$, the minimal average entropy can only be attained in the set of $\overline{\mathscr{S}}_{\min} = \min\left\{\overline{\mathscr{S}}_{\leftrightarrow}(r_z), \overline{\mathscr{S}}_{\updownarrow}(r_z)\right\}$, whose optimal measurements on $\mathscr{B}$ correspond to the observation of either σ_x or σ_z.

Let us now turn to the discussion of a non-trivial case that the center of E departs from the origin O in the x–z plane, three-element POVM measurements will be introduced by means of the geometric picture approaches.[30,37] Given an E with $z_0 \neq 0$ (i.e., $\rho_{11}\rho_{22} \neq \rho_{33}\rho_{44}$), one can use LFO to move the point A along the z axis and leaves E unchanged.[30] It is possible that the z coordinate of the moving point A corresponding to a certain value z_T makes $\overline{\mathscr{S}}_{\leftrightarrow}(z_T)$ and $\overline{\mathscr{S}}_{\updownarrow}(z_T)$ be exactly equal as shown in Fig. 2(a). The two functions of $\overline{\mathscr{S}}_{\leftrightarrow}(r_z)$ and $\overline{\mathscr{S}}_{\updownarrow}(r_z)$ only have a crossing point if ignoring the two points of G and H. It has been shown that the entropy function $\overline{\mathscr{S}}_{\leftrightarrow}(r_z)$ has at most one inflection point.[37] As shown in Fig. 2(a), one can always draw a straight line $L_{\mathscr{Z}G}$ passing through its right end point G tangent to the function curve $\overline{\mathscr{S}}_{\leftrightarrow}(r_z)$, in which $L_{\mathscr{Z}G}$ has a tangent point corresponding to a point $\mathscr{Z} = (0, z_\Delta)$ on the z axis. The tangent line $L_{\mathscr{Z}G}$ with $z_T \in (z_\Delta, z_G)$ can make it possible to obtain a smaller average entropy than that given by $\overline{\mathscr{S}}_{\updownarrow}$ or $\overline{\mathscr{S}}_{\leftrightarrow}$ corresponding to the dashed blue and real black lines. The $L_{\mathscr{Z}G}$ gives a convex combination of three entropy functions corresponding to $h(\overline{OE})$, $h(\overline{OF})$, and $h(\overline{OG})$, respectively, as described in the context and illustrated in Fig. 1(a). The decomposed states induced by various choices from POVM elements of $\{M_i^{\mathscr{B}}\}$ can be directly shown by E, on which three points are distributed symmetrically. The average entropy can be given by

$$\begin{aligned} \overline{\mathscr{S}}_{\Delta} &= p_G\mathscr{S}(\rho_G) + p_E\mathscr{S}(\rho_E) + p_F\mathscr{S}(\rho_F) \\ &= p_G h(\overline{OG}) + p_E h(\overline{OE}) + p_F h(\overline{OF}), \end{aligned} \tag{17}$$

where $\overline{OE} = \overline{OF} = \sqrt{z_\Delta^2 + \ell_1^2\,[\ell_3^2 - (z_\Delta - z_0)^2]/\ell_3^2}$, $p_G = \overline{A\mathscr{Z}}/\overline{G\mathscr{Z}}$, and $p_E = p_F = (1/2)(\overline{GA}/\overline{G\mathscr{Z}})$. The authors[37] have pointed out that if the coordinate of local state ρ_A lies in the range of $z_\Delta < r_z < z_G$, three-element decomposition will

give rise to a more optimal average entropy. As shown in Fig. 2(a), the minimal average entropy given by the point M on the tangent line $L_{\mathscr{Z}G}$ is smaller than that by point N.

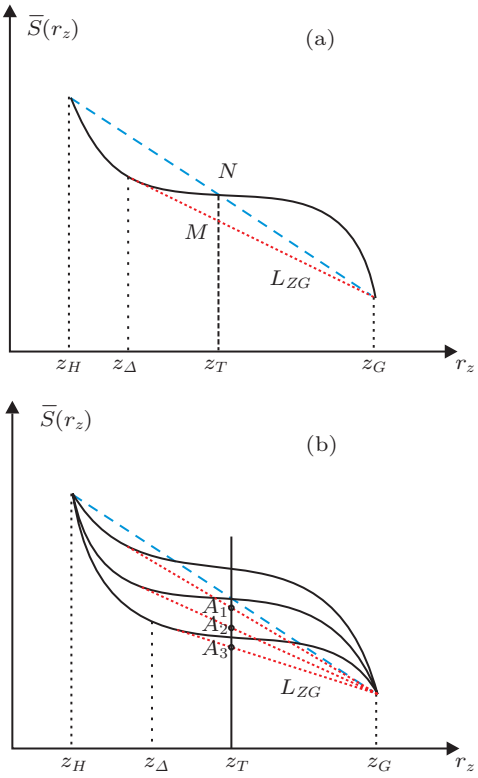


Fig. 2. (color online) For a fixed E, a moving point A corresponds to the ρ_A along the z axis by LFO. Blue dashed line and black real line represent two functions of $\overline{\mathscr{S}}_{\updownarrow}(r_z)$ and $\overline{\mathscr{S}}_{\leftrightarrow}(r_z)$ respectively. The two functions intersecting at the point N make $\overline{\mathscr{S}}_{\updownarrow} = \overline{\mathscr{S}}_{\leftrightarrow}$. One can draw a tangent line $L_{\mathscr{Z}G}$ with $z_T \in (z_\Delta, z_G)$, in which the average entropy can access a smaller value than that given by $\overline{\mathscr{S}}_{\updownarrow}$ and $\overline{\mathscr{S}}_{\leftrightarrow}$ corresponding to the dashed blue and real black lines. (b) In the PD channel, the shrinking E will make the value of the function $\overline{\mathscr{S}}_{\leftrightarrow}(r_z)$ increase. From top to bottom, three real black lines corresponding to different evolution time $t_0+\delta t, t_0$, and $t_0-\delta t$ show that the $\overline{\mathscr{S}}_{\Delta}$ increases continuously for a certain z-axis coordinate z_T of the local state. For a certain point $(0, z_T)$ of the local state, A_1, A_2, and A_3 respectively correspond to optimal average entropy of different time instants of decoherence evolution under the POVM measurements.

5. The dynamics of quantum discord

In terms of the three-element POVM measurements, we set out to study the dynamical evolution of discord of the X states and reinvestigate the sudden change. Specifically, we shall introduce a typical kind of unital noise channel,[4] i.e., phase damping (PD) channel, which is a decoherence model with no energy exchange between the system and environment. This channel can take the identity operator to itself so that $\mathscr{E}(\mathbb{I}/2) = \mathbb{I}/2$ and preserve any component of the Bloch vector in the σ_z direction, while shrinking any one in the σ_x and σ_y directions. Specifically, the PD channel can be described by a complete set of Kraus operators $\{K_i\}$ satisfying normalization condition $\sum_{\mu=1}^{2} K_\mu^\dagger K_\mu = \mathbb{I}$, and in the computational basis it has the following form of

$$K_1 = |0\rangle\langle 0| + \sqrt{1-\gamma}|1\rangle\langle 1|,$$

$$K_2 = \sqrt{\gamma}|1\rangle\langle 1|, \tag{18}$$

where γ represents the decay rate as a function of time t. There is an associated two-sided quantum map $\mathscr{E}_{\mathscr{A}\mathscr{B}}$ that transforms initial quantum state $\rho_{\mathscr{A}\mathscr{B}}$ to

$$\mathscr{E}_{\mathscr{A}\mathscr{B}}(\rho_{\mathscr{A}\mathscr{B}}) = \sum_{i,j=1}^{2} (K_i \otimes K_j)\rho_{\mathscr{A}\mathscr{B}}(K_i^\dagger \otimes K_j^\dagger). \tag{19}$$

In the PD channel, equation (5) is transformed to the form of

$$\frac{x^2}{(1-\gamma)^2\ell_1^2} + \frac{y^2}{(1-\gamma)^2\ell_2^2} + \frac{(z-z_0)^2}{\ell_3^2} = 1. \tag{20}$$

On the scaled down surface of the $\mathfrak{E}$, each point shrinks to the z axis. Without loss of generality, one only needs to consider the E in the x–z plane as shown in Fig. 1(a).

Remark 2 For the X states with $\rho_{11}\rho_{22} = \rho_{33}\rho_{44}$ satisfying $\ell_1 > \ell_3$, when passing through the PD channels, the dynamics of discord and classical correlations will exhibit a sudden change.

The PD channels keep the center coordinate O and $\overline{GH}$ of E fixed, therefore, with Remark 1, the $\overline{\mathscr{S}}_{\min}$ can only be obtained by two alternative decompositions, i.e., horizontal and vertical ones. Thus, the sudden change of chosen optimal decomposition leads to the sudden change of dynamical evolution. Obviously, the Bell-diagonal states are included in this result.

Remark 3 For a family of initial X states with $\rho_{11}\rho_{22} \neq \rho_{33}\rho_{44}$ and $\overline{\mathscr{S}}_{\leftrightarrow} > \overline{\mathscr{S}}_{\updownarrow}$, at a time instant the sudden change derived from orthogonal measurements should have happened, three-element POVM measurements may make them evolve smoothly without any abrupt change and give more optimal quantities of discord during the decoherence process.

For the decay rate $\gamma(t)$, the time instant t_0 of $\overline{\mathscr{S}}^{t_0}_{\leftrightarrow}$ equalling to $\overline{\mathscr{S}}^{t_0}_{\updownarrow}$, for which the two functions of $\overline{\mathscr{S}}_{\leftrightarrow}(r_z)$ and $\overline{\mathscr{S}}_{\updownarrow}(r_z)$ induced again by LFO moving the point A along the z axis have a crossing point corresponding to the moment t_0 of sudden change. [Note that we use the symbol t_0 as superscript to label the time instant of decay rate.] There is a tangent line segment $L_{\mathscr{Z}G}$, as pictured in Fig. 2, that can give a more optimal minimal average entropy $\overline{\mathscr{S}}_{\Delta}$. For an adjacent evolution time instant $t_0 \mp \delta t$ of the t_0, we must have an inequality of $\overline{\mathscr{S}}^{t_0-\delta t}_{\leftrightarrow}(R_z) < \overline{\mathscr{S}}^{t_0}_{\leftrightarrow}(R_z) < \overline{\mathscr{S}}^{t_0+\delta t}_{\leftrightarrow}(R_z)$, since the $\overline{GH}$ and the Bloch vector $(0, R_z)$ of the reduced state ρ_A are fixed in the PD channel. For each time instant, one can always move the local state ρ_A by LFO along the z axis from G to H (H to G), and define the two functions of $\overline{\mathscr{S}}_{\leftrightarrow}(r_z)$ and $\overline{\mathscr{S}}_{\updownarrow}(r_z)$. One can still obtain the inequality $\overline{\mathscr{S}}^{t_0-\delta t}_{\leftrightarrow}(r_z) < \overline{\mathscr{S}}^{t_0}_{\leftrightarrow}(r_z) < \overline{\mathscr{S}}^{t_0+\delta t}_{\leftrightarrow}(r_z)$. Figure 2(b) schematically illustrates a continuous series of the functional curves of $\overline{\mathscr{S}}_{\leftrightarrow}(r_z)$ with the continuous change of time for $\delta t \to 0$ in the PD channel . For the local state of ρ_A with the fixed Bloch vector $(0, R_z)$ in E, the minimal average entropy of $\overline{\mathscr{S}}^{t}_{\Delta}(R_z)$ given by the tangent line $L_{\mathscr{Z}G}$ rises continuously over time t.

A concrete example of dynamical behaviour is revealed by Fig. 1(b) to show that the entire evolution process from classical to quantum decoherence is smooth and does not manifest any sudden change. In Fig. 1(c), the value z_Δ corresponding to z axis coordinate of point $\mathscr{Z}$ decreases continuously from point A to lower vertex H with the shrinking E. Within the interval of $0.4731 \leq \gamma(t) \leq 0.4737$, the optimal decomposition has three-element states corresponding to the POVM measurements. In the situation where $\gamma(t) < 0.4731$ or $\gamma(t) > 0.4737$, the optimal measurements are equivalent to two-element orthogonal measurements corresponding to either σ_x or σ_z. Finally, it should be noted that the two-element orthogonal measurement has been able to give a good approximation of the discord, and there is only a subset of X states for which numerics shows their tiny differences.[33,36] However, the tiny differences may make an essential distinction for the decoherence process.

6. Conclusion

In this work, we have combined the convex analysis with the geometric picture of the available decomposition of local state in the steering ellipsoid, and proved that choosing the three-element POVM measurements instead of two-element orthogonal measurements can give more optimal quantities of discord for a family of X states. Furthermore, by means of the three-element POVM measurements we presented that, except for those initial states with $\rho_{11}\rho_{22} = \rho_{33}\rho_{44}$, there does not exist any sudden change for a family of X states under the phase damping channel. One interesting conclusion is that the decoherence of some initial states with the sudden transition character becomes a smooth transition due to more optimal three-element POVM measurements. The physical mechanics of the sudden and smooth transition may be valuable for further considerations. In addition, the revised measure of discord defined by the three-element POVM measurements can be used to reinvestigate the correlation dynamics of a composite system under the dissipative environments, and may reveal the conditions of presence or absence of the sudden change points compared to that given by two-element orthogonal measurements.

References

[1] Bennett C H, DiVincenzo D P, Fuchs C A, Mor T, Rains E, Shor P W, Smolin J A and Wootters W K 1999 *Phys. Rev. A* **59** 1070
[2] Henderson L and Vedral V 2001 *J. Phys. A: Math. Gen.* **34** 6899
[3] Ollivier H and Zurek W H 2001 *Phys. Rev. Lett.* **88** 017901
[4] Nielsen M A and Chuang I L 2000 *Quantum Computation and Quantum Information* (Cambridge: Cambridge University Press)
[5] Knill E and Laflamme R 1998 *Phys. Rev. Lett.* **81** 5672
[6] Datta A, Shaji A and Caves C M 2008 *Phys. Rev. Lett.* **100** 050502
[7] Piani M, Horodecki P and Horodecki R 2008 *Phys. Rev. Lett.* **100** 090502
[8] Cavalcanti D, Aolita L, Boixo S, Modi K, Piani M and Winter A 2011 *Phys. Rev. A* **83** 032324
[9] Zurek W H 2003 *Phys. Rev. A* **67** 012320
[10] Vedral V 2010 *Found. Phys.* **40** 1141
[11] Modi K, Cable H, Williamson M and Vedral V 2011 *Phys. Rev. X* **1** 021022
[12] Horodecki M, Horodecki P, Horodecki R, Oppenheim J, SensDed A, Sen U and Radtke B S 2005 *Phys. Rev. A* **71** 062307
[13] Dakic B, Vedral V and Brukner C 2010 *Phys. Rev. Lett.* **105** 190502
[14] Luo S and Fu S 2010 *Phys. Rev. A* **82:** 034302.
[15] Jiang F J, Lu H J, Yan X H and Shi M J 2013 *Chin. Phys. B* **22** 040303
[16] Tang H J, Liu Y M, Chen J L, Ye B L and Zhang Z J 2013 *Int. J. Quantum Inform.* **9** 981
[17] Modi K, Paterek T, Son W, Vedral V and Williamson M 2010 *Phys. Rev. Lett.* **104** 080501
[18] Fanchini F F, Werlang T, Brasil C A, Arruda L G E and Caldeira A O 2010 *Phys. Rev. A* **81** 052107
[19] Maziero J, Werlang T, Fanchini F F, Celeri L C C and Serra R M 2010 *Phys. Rev. A* **81** 022116
[20] Werlang T, Souza S, Fanchini F F and Boas C J V 2009 *Phys. Rev. A* **80** 024103
[21] Xu G F and Tong D M 2011 *Chin. Phys. Lett.* **28** 060305
[22] Werlang T, Trippe C, Ribeiro G A P and Rigolin G 2010 *Phys. Rev. Lett.* **105** 095702
[23] Mazzola L, Piilo J and Maniscalco S 2010 *Phys. Rev. Lett.* **104** 200401
[24] Mazzola L, Piilo J and Maniscalco S 2011 *Int. J. Quantum Inform.* **9** 981
[25] Xu J S, Xu X Y, Li C F, Zhang C J, Zou X B and Guo G C 2010 *Nat. Commun.* **1** 7
[26] Aaronson B, Franco R L and Adesso G 2013 *Phys. Rev. A* **88** 012120
[27] Rong X, Wang Z X, Jin F Z, Geng J P, Feng P B, Xu N Y, Wang Y, Ju C Y, Shi M J and Du J F 2012 *Phys. Rev. B* **86** 104425
[28] Rong X, Jin F Z, Wang Z X, Geng J P, Ju C Y, Wang Y, Zhang R M, Duan C K, Shi M J and Du J F 2013 *Phys. Rev. B* **88** 054419
[29] Streltsov A, Kampermann H and BruB D 2011 *Phys. Rev. Lett.* **107** 170502
[30] Shi M J, Jiang F J, Sun C X and Du J F 2011 *New J. Phys.* **13** 073016
[31] Luo S 2008 *Phys. Rev. A* **77** 042303
[32] Ali M, Rau A R P and Alber G 2010 *Phys. Rev. A* **81** 042105
[33] Lu X M, Ma J, Xi Z J and Wang X G 2011 *Phys. Rev. A* **83** 012327
[34] Girolami D and Adesso G 2011 *Phys. Rev. A* **83** 052108
[35] Jevtic S, Pusey M, Jennings D and Rudolph T 2014 *Phys. Rev. Lett.* **113** 020402
[36] Chen Q, Zhang C J, Yu S X, Yi X X and Oh C H 2011 *Phys. Rev. A* **84** 042313
[37] Shi M J, Sun C X, Jiang F J and Du J F 2011 *Phys. Rev. A* **85** 064104
[38] Shi M J, Jiang F J and Du J F 2011 q-ph arXiv: 1107.4457v1
[39] Verstraete F, Dehaene J and DeMoor B 2001 *Phys. Rev. A* **64** 010101
[40] Shi M J, Yang W, Jiang F J and Du J F 2011 *J. Phys. A: Math. Theor.* **44** 415304
[41] Verstraete F 2002 "A Study Of Entanglement in Quantum Information Theory", Ph. D. Thesis (Leuven: Katholieke University) (in Belgium)